Naphthalene Adsorption and Desorption from Aqueous C_{60} Fullerene

Xuekun Cheng,* Amy T. Kan, and Mason B. Tomson

Department of Civil and Environmental Engineering, Rice University, MS 519, 6100 Main Street, Houston, Texas 77005

The main purpose of this study was to characterize the adsorption and desorption interactions of naphthalene, a model environmental organic pollutant, with C_{60} fullerene. C_{60} fullerene was used as a model adsorbent for carbonaceous nanoparticles. Typical batch reactors were used to perform adsorption and desorption experiments. Adsorption and desorption of naphthalene to and from C_{60} fullerene solids in different aggregation forms was studied, where C_{60} was used as purchased, deposited as a thin film, or dispersed in water by magnetic mixing. Adsorption and desorption of naphthalene to activated carbon, a common sorbent, was also studied and compared with that of C_{60}. It was found in this study that the enhanced dispersal of C_{60} could affect the adsorption of naphthalene by several orders of magnitude. A solid-water distribution coefficient of $10^{2.4}$ mL·g^{-1} was obtained for adsorption of naphthalene to poorly dispersed C_{60}, whereas ($10^{4.2}$ to $10^{4.3}$) ml·g^{-1} coefficients were obtained for well-dispersed C_{60} samples. In addition, desorption of naphthalene from dispersed C_{60} samples into aqueous solutions was found to exhibit strong hysteresis. For the desorption over a period of 60 days, only about 11% of total naphthalene was desorbed from C_{60}. Possible mechanisms for these observations are discussed.

Introduction

Fullerenes have been of great interest to scientists in many different areas since their first discovery.[1] The unique chemical and physical properties of carbonaceous nanomaterials have driven researchers to find more and more potential applications for them including their use in environmental remediation. Numerous nanomaterials have been synthesized by companies all over the world. If these materials are produced and used in large amounts, their release into the environment, including the atmosphere, hydrosphere, and biosphere, will become inevitable. Carbonaceous nanomaterials such as fullerenes could possibly transport with groundwater in aquifer systems, deposit to soils or sediments, be taken up by microorganisms or plants, or even be inhaled by human beings. Therefore, understanding of the fate and transport of those nanomaterials in the environment is critical.

It's well known that carbon in numerous forms is found in atmospheric aerosols, estuarine, sediments, and soils, where its influence on transport and bioavailability of pollutants, especially organic pollutants, is of great concern. It has been shown that the presence of high surface area carbonaceous materials in the soils and sediments can affect the adsorption of organic hydrocarbons to soils and sediments.[2−5] Soot, residues of incomplete combustion, has been found to significantly enhance the sorption of hydrophobic organic compounds to soils and sediments[4,6] and contributes to the sequestration of organic contaminants.[5] Other carbonaceous materials such as coal or charcoal residues in aquifer systems have also been claimed to enhance the sorption of organic compounds to soils. On the other hand, it has been reported that the existence of dissolved or colloidal organic matter could enhance the partition of neutral organic contaminants into water and thus enhance the transport of these compounds.[7−9] It was shown that, if the concentration of dissolved or colloidal organic matter reaches some critical level, all organic compounds with K_{ow} values above a specific value could move at the same rate as groundwater. In some situations, the movements of highly hydrophobic compounds could be enhanced by a factor of a thousand or more.[9] It is unknown whether the release of C_{60} fullerene and other nanosized carbonaceous nanomaterials into the environment will either enhance the sorption of organic contaminants and thus reduce their mobility or enhance the transport of those compounds. Therefore, it is of great importance to study the adsorptive interactions of carbonaceous nanomaterials with environmental contaminants.

A few research groups have explored the adsorptive properties of fullerenes. Most of them have focused on the adsorption of simple gases or vapors of organic compounds on C_{60} solid.[10−16] Only few studies[17,18] dealt with the interfacial interactions of environmental organic contaminants with C_{60} in aqueous media. Fullerenes exhibit strong hydrophobicity in aqueous media. Various methods have been used to disperse fullerenes in aqueous media, for example, sonication,[19] interaction with polymers,[20] redox reactions,[21] or extended mixing (this study). Many of these processes may occur either during the manufacture of fullerene-containing nanomaterials or as a natural process in the environment, for instance, those mediated by microorganisms, flow, time, etc. In this paper, the adsorption of naphthalene, a common organic contaminant, to C_{60} dispersed to different degrees in aqueous solution is discussed.

Adsorption/desorption hysteresis is one phenomenon that has been observed in many adsorption studies for organic hydrocarbons to soils and sediment.[22−36] When desorption is not the opposite of the adsorption process and there is a specific amount of the adsorbed organic compounds resistant to desorption, the desorption is referred to as hyster-

* To whom correspondence may be addressed. Phone: (713) 348-2026. E-mail: xkcheng@rice.edu.

10.1021/je030247m CCC: $27.50
Published on Web 04/06/2004

Table 1. Experimental Setups

exp	type	solution matrix	solid/solution ratio	mixing	procedures
1	naphthalene adsorption to "C_{60} large aggregates"	0.01 M NaCl, 0.01 M NaN_3	5 mg C_{60}, 23 mL solution	rotation, end over end	"C_{60} large aggregates" suspended in 4 naphthalene/electrolyte solutions at different concentrations → rotate for 3 days → filter → measure C_w
2	naphthalene adsorption to activated carbon	0.01 M NaCl, 0.01 M NaN_3	2 mg activated carbon, 40 mL solution	rotation, end over end	procedure same as exp 1 with 5 concentrations of naphthalene/electrolyte solutions and 3 different temperatures
3	naphthalene adsorption to "C_{60} thin film"	0.01 M NaCl, 0.01 M NaN_3	10 mg C_{60}, 40 mL solution	rotation, end over end	evaporation of C_{60}/CH_2Cl_2 solution → add 5 concentrations of naphthalene/electrolyte solutions → rotate for 3 days → filter → measure C_w
4	naphthalene desorption from "C_{60} thin film"	0.01 M NaCl, 0.01 M NaN_3	0.5 mg C_{60}, 40 mL solution	rotation, end over end	evaporation of C_{60}/naphthalene/CH_2Cl_2 solution → add electrolyte solutions → rotate for 3 days → filter → measure C_w
5	successive adsorption/desorption of naphthalene to/from "C_{60} small aggregates"	0.01 M NaCl, 0.01 M NaN_3	21−24 mg C_{60}, 28 mL solution	magnetic stirring	C_{60} stirred in 30 mL electrolyte solution for 2 days → successive injection of naphthalene standard solution at 2 days interval → centrifugation and sampling every 2 days → centrifugation and decantation → multistep desorption

esis. Hysteresis was found in the preparation of C_{60} [37] and in the adsorption of cyclopentane vapor to C_{60} powders.[11,12] This phenomenon of hysteresis has also been found in this study and will be discussed.

Polynuclear aromatic hydrocarbons (PAHs) represent a class of nonionic, hydrophobic, and toxic organic compounds that occur in environmental matrixes due to numerous causes. PAHs are an important class of environmental pollutants because of their notable amounts in the environment, their toxicological risks, and their strong persistence in soils and sediments. The transport, partitioning, and bioavailability of PAHs as contaminants in groundwater and surface waters are known to be highly dependent on the interactions of these compounds with soil organic matter and mobile colloids, which are largely composed of humic substances. The bioavailability of these contaminants to degrading micro-organisms has been closely linked to soil organic matter.[38,39] The amount of organic carbon and the hydrophobicity of soil organic matter were estimated to be the most significant parameters in decreasing the environmental availability of PAHs.[2,40,41] In this study, naphthalene, the simplest form of PAHs, was selected as a model organic contaminant.

Materials and Methods

Materials. C_{60} fullerene with purity > 99.5% was obtained from Aldrich. The fullerene sample was used without further purification. Activated carbon (D/S React-C) was obtained from Calgon Carbon Corp. (Pittsburgh, PA). Activated carbon samples were pulverized with a pestle and mortar and sieved with a 75-μm sieve before use.

^{14}C-radiolabeled naphthalene with a specific activity of 8.1 μCi/μmol (Sigma−Aldrich, St. Louis, MO) was prepared in methanol (HPLC grade). Toluene used in the experiments was from Sigma−Aldrich with a purity of 99.8%. Methylene chloride was ACS reagent grade (Fisher Scientific.). Ready-Safe or Ready Organic liquid scintillation cocktails for scintillation counting were supplied by Beckman Instruments, Inc. (Fullerton, CA).

Electrolyte solution used to conduct adsorption and desorption experiments was prepared in deionized water with sodium chloride (Fisher Scientific, biological grade) and sodium azide (Eastman Kodak, >98%, see Table 1). Sodium azide was used to inhibit bacterial growth.

Methods. Five different adsorption/desorption experimental protocols were used in this study to determine the adsorption of naphthalene to C_{60} fullerene, which was dispersed to different degrees (see below). Experimental parameters for the adsorption/desorption experiments with C_{60} fullerene or activated carbon are listed in Table 1.

Adsorption of Naphthalene from Aqueous Solution to "C_{60} Large Aggregates". For experiment 1, 1 mg/mL C_{60} suspension was prepared by mixing (100 ± 0.1) mg of C_{60} fullerene in a beaker containing 100 mL of electrolyte solution. Five milliliters of C_{60} suspension was added into each of the four 23-mL glass vials. Then ^{14}C-radiolabeled naphthalene/methanol stock solutions were injected into the four vials with a microsyringe (Hamilton, Hamilton Company, Reno, Nevada) so that the initial naphthalene concentrations were (0.94, 1.91, 2.61, 3.72) μg/mL, respectively. The analysis of each sample of unknown concentration was repeated three times. The uncertainty of the initial naphthalene concentrations was less than ±0.02 μg/mL, estimated by the standard deviation of the three replicated measurements. After filling with naphthalene electrolyte solutions, the headspace in each vial was typically less than 0.1 mL. The volume fraction of methanol in solution phase in each vial was less than 0.004, which was not expected to affect the naphthalene adsorption. The vials were sealed with Teflon-septum caps and rotated end-over-end at about 1 rpm at room temperature for 3 days. Another four control vials were set up the same way as the four corresponding samples described above, except that no C_{60} fullerene was added. At the end of the time period, samples and controls were filtered with 0.02-μm inorganic membrane filters (Anotop, Whatman Inc., Clifton, NJ) and the filtrates were analyzed with a liquid-scintillation counter (Beckman Instruments Inc., Fullerton, CA). The average sorption of naphthalene to the membrane filters was determined in a preliminary study to be 8.0%, with a standard error of ±0.4%. Thus, for those samples in which inorganic filters were used, the experimentally measured aqueous concentrations of naphthalene were corrected (by dividing the

measured concentrations by 0.92) for the sorption to the filters. Solid-phase naphthalene concentrations were calculated from the differences between the solution-phase concentrations in the sample vials and that in the corresponding control vials.

Adsorption of Naphthalene from Aqueous Solution to Activated Carbon. In experiment 2, 40-mL activated carbon suspensions containing (2 ± 0.1) mg of activated carbon were used instead of C_{60} suspensions. Operation for this set of experiments was similar to that of experiment 1. Initial naphthalene concentrations were (0.89, 1.84, 2.78, 3.63, 4.78) μg/mL, respectively, in five sample vials. The uncertainty of the initial naphthalene concentrations was less than ±0.02 μg/mL. Adsorption to activated carbon was conducted at (298 ± 0.1, 311 ± 0.1, and 328 ± 0.1) K to evaluate isosteric heats for naphthalene adsorption and to validate experimental protocol with literature observations.

Adsorption/Desorption of Naphthalene to/from "C_{60} Thin Film". In experiment 3 (adsorption), C_{60} fullerene powders were first dissolved in methylene chloride at a concentration of (0.1 ± 0.001) mg/mL. In each of the five 40-mL glass vials, 100 mL of C_{60}/methylene chloride solution was added and a Kuderna−Danish concentrator was used to remove the solvent. When the methylene chloride was completely evaporated, a film of C_{60} fullerene (10 ± 0.1 mg) was formed on the internal walls of the vials. ^{14}C-radiolabeled naphthalene/electrolyte solutions at five different concentrations of (0.97, 1.80, 2.95, 3.87, 5.04) μg/mL were added into the vials leaving less than 0.1 mL headspace, and the vials were sealed tightly with Teflon-septum caps and rotated end-over-end at about 1 rpm at room temperature for 3 days. The uncertainty of the initial naphthalene concentrations was less than ±0.6%. At the end of the time period, samples were filtered with 0.02-μm inorganic membrane filters (Anotop, Whatman Inc., Clifton, NJ) and the filtrates were analyzed in a liquid-scintillation counter (Beckman Instruments Inc., Fullerton, CA). At the end of the adsorption experiments, C_{60} fullerene was dissolved in toluene and was analyzed for naphthalene by GC-MS (Hewlett-Packard 6890 GC, Hewlett-Packard 5973 Mass Selective Detector) to check the mass balance.

In experiment 4 (desorption), 10 mL of (0.05 ± 0.001) mg C_{60} per milliliter methylene chloride solution was added to each of the five 40-mL sample vials, rendering the C_{60} amount in each vial to be (0.5 ± 0.01) mg. Next, 2 μL, 10 μL, 40 μL, 70 μL, and 90 μL of (1900 ± 0.1) μg/mL ^{14}C-radiolabeled naphthalene standard solution was injected into C_{60}/methylene chloride solutions in the five sample vials, respectively, with a microsyringe (Hamilton, Hamilton Company, Reno, Nevada). After the addition of naphthalene solutions, the solution in each sample vial was heated in a Kuderna−Danish concentrator at (318 ± 1) K to remove methylene chloride. Kuderna−Danish concentrators were used to minimize the loss of naphthalene during evaporation of methylene chloride. At the end of the evaporation, there was less than 0.02 mL of methylene chloride left in each sample vial, determined by final weight. At the end of the methylene chloride evaporation, it was assumed that naphthalene was associated with the "C_{60} thin film", although it could not be proven by direct measurement. Then naphthalene-free electrolyte solutions were added into the five sample vials to induce desorption. The vials were sealed with Teflon-septum caps and rotated end-over-end at about 1 rpm at room temperature for 3 days for desorption equilibrium. After desorption, solutions were filtered with 0.02-μm inorganic membrane filters (Anotop, Whatman Inc., Clifton, NJ) and concentrations were determined with a scintillation counter (Beckman Instruments Inc., Fullerton, CA). The solid-phase naphthalene concentrations were measured by dissolving the C_{60} fullerene in toluene and by GC/MS (Hewlett-Packard 6890 GC, Hewlett-Packard 5973 Mass Selective Detector) analysis.

Table 2. Experimental Adsorption Isotherm Data for Naphthalene Adsorption to "C_{60} Large Aggregates"

C_w / μg·mL^{-1}	q / μg·g^{-1}
0.88	260
1.78	498
2.46	561
3.49	844

Adsorption/Desorption of Naphthalene to/from "C_{60} Small Aggregates". For experiment 5, (21 ± 0.1, and 24 ± 0.1) mg of C_{60} fullerene was added into two 28-mL glass centrifuge vials (sample nos. 5.1 and 5.2). A magnetic Teflon-coated stirring bar was put in each vial. The two sample vials were then filled with electrolyte solutions (with ~0.1 mL headspace) and were sealed with Teflon-septum caps. Sample vials were stirred on a magnetic stirrer (Fisher Scientific) at about 1000 rpm at room temperature for 2 days to disperse C_{60} fullerene. Adsorption was then induced by injecting (10.0 and 17.5) μL of ^{14}C-radiolabeled naphthalene stock solution (4990 ± 0.1 μg/mL) into the two sample vials, respectively. At the end of each adsorption step, 1 mL of supernatant was sampled after centrifugation at 6000 rpm (IEC Centra MP4 Centrifuge, International Equipment) and analyzed with a scintillation counter. Successive adsorption steps were accomplished by adding identical aliquots of naphthalene stock solution and additional electrolyte solution (about 1 mL each time) to the vial to fill the headspace. Five or six adsorption steps were performed with the two samples; the time interval between adsorption steps was 2 days. At the end of the last adsorption step, multistep desorption was induced by centrifugation and successively replacing each supernatant solution with naphthalene-free solution. The time intervals between desorption steps varied from 2 to 27 days. At the end of each desorption step, the solution-phase naphthalene concentration was analyzed by scintillation counting.

UV−vis Spectrophotometer Analysis. C_{60} in the C_{60}/water mixture was sampled after 2 days mixing and dissolved in toluene. C_{60} in toluene solution was analyzed by UV−vis spectrophotometer (Cary 400) to confirm the chemical state of C_{60} in the mixture.

Scanning Electron Microscopy (SEM) Analysis. C_{60} aggregates used in experiments 1 and 5 were analyzed by SEM (FEI XL-30 ESEM) to confirm the formation of C_{60} aggregation and estimate the sizes of C_{60} aggregates.

Results and Discussion

Adsorption of Naphthalene from Aqueous Solution to "C_{60} Large Aggregates". The adsorption equilibrium data of naphthalene to "C_{60} large aggregates" via the protocol of experiment 1 are presented in Table 2. The accuracy of the concentration measurements by scintillation counting was set to be less than ±0.5%. The analysis of each sample was repeated at lease three times, and standard deviation was calculated based on the replicates. The uncertainty of the final solution-phase naphthalene concentrations was calculated to be less than ±0.05 μg/mL. Adsorption data were fitted with a linear isotherm and are presented in Figure 1. The term "C_{60} large aggregates"

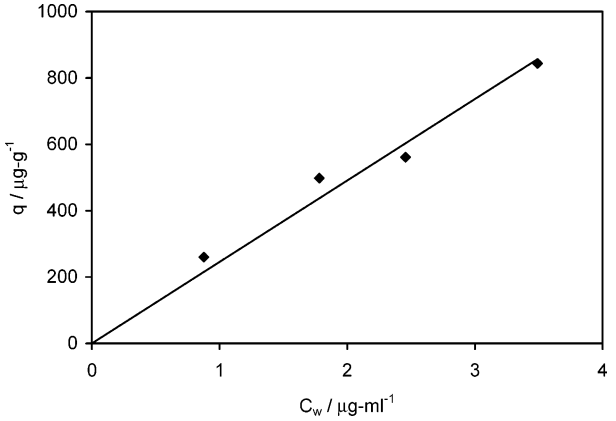

Figure 1. Plot of experimental data of naphthalene adsorption to "C_{60} large aggregates" (experiment 1). ◆, Experimental data; solid line, linear isotherm.

is used to refer to the C_{60} black powder purchased from Sigma−Aldrich and suspended in electrolyte solution. From SEM examination (micrographs not included), the diameters of these well-formed particulate aggregates were observed to be from (20 to 50) μm. At equilibrium, the solution-phase concentrations decreased by as little as 4.50% to 6.51%, indicating that very little naphthalene was adsorbed to C_{60} fullerene. A linear isotherm in the form of $q = K_pC_w$ was observed, where K_p/mL·g^{-1} denotes the partition coefficient,[42] q/μg·g^{-1} is the mass of naphthalene per unit mass of C_{60} at equilibrium, and C_w/μg·mL^{-1} is the naphthalene concentration in the solution phase at equilibrium. A K_p value of ($10^{2.39} \pm 10.73$) mL·g^{-1} is obtained from data in Table 2 and Figure 1. Since C_{60} presents a very hydrophobic surface, it was expected that C_{60} could be a preferred sorbent for many common organic compounds and adsorption to C_{60} was expected to be comparable to that on activated carbon, a commonly used adsorbent. However, the observed K_p value is much smaller than expected. Ballesteros and co-workers[18] reported the chromatographic separation of organic compounds from aqueous solutions by C_{60} particles in a column study. By use of their data, a partition coefficient 1 order of magnitude smaller than that found in experiment 1 was calculated.

Adsorption of Naphthalene from Aqueous Solution to Activated Carbon. To compare the adsorption properties of carbonaceous materials, activated carbon was tested as a reference sorbent. The same experimental procedure was used, except that adsorption experiments for activated carbon were conducted at three different temperatures (experiment 2). In each of the five samples, even though the solid/solution ratio for activated carbon was less than one-fourth of that for "C_{60} large aggregates" (experiment 1), over 95% of naphthalene was adsorbed from electrolyte solution to activated carbon at equilibrium. Solution-phase naphthalene concentrations and solid-phase naphthalene concentrations at adsorption equilibrium are presented in Table 3. Mean values of coefficients of variation for the final solution-phase naphthalene concentrations was ± 1.0%, calculated based on three replicates for each sample. Adsorption data were fitted with Freundlich isotherms and are presented in Figure 2. Freundlich equations in the form of $q = K_FC_w^n$ were used to describe the isotherms. In the Freundlich equation, K_F is the Freundlich constant, n is the Freundlich exponent, q/μg·g^{-1} is the mass of naphthalene per unit mass of sorbent at equilibrium, and C_w/μg·mL^{-1} is the naphthalene concentration in the solution phase at equilibrium. Values of the Freundlich parameters are listed in Table 4. Values of the standard deviation, the

Table 3. Experimental Adsorption Isotherm Data for Naphthalene Adsorption to Activated Carbon at Three Different Temperature (T/K)

T = 298 K		T = 311 K		T = 328 K	
C_w	q	C_w	q	C_w	q
μg·mL^{-1}	μg·g^{-1}	μg·mL^{-1}	μg·g^{-1}	μg·mL^{-1}	μg·g^{-1}
0.002	19571	0.002	19560	0.004	19512
0.009	38795	0.014	38677	0.034	38253
0.034	58560	0.056	58131	0.127	56591
0.113	75379	0.161	74318	0.349	70273
0.229	97524	0.321	95453	0.616	89022

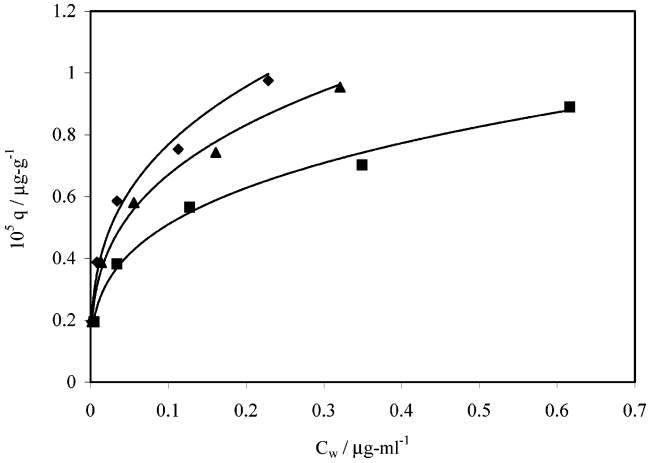

Figure 2. Plot of experimental data of naphthalene adsorption to activated carbon at three different temperatures. ◆, Adsorption data at 298 K; ▲, adsorption data at 311 K; ■, adsorption data at 328 K; solid line, Freundlich isotherms.

Table 4. Freundlich Parameters for Naphthalene Adsorption to Activated Carbon at Different Temperatures (T/K)

T/K	K_F [a]	n[b]	R^2 [e]
298	$10^{5.17} \pm 10^{3.91}$ [c] (5.5%)[d]	0.29 ± 0.02[c] (7.2%)[d]	0.985
311	$10^{5.12} \pm 10^{3.67}$ (3.5%)	0.30 ± 0.02 (5.3%)	0.993
328	$10^{5.00} \pm 10^{3.48}$ (3.0%)	0.29 ± 0.02 (6.3%)	0.993

[a] Freundlich constant. [b] Freundlich exponent. [c] Standard deviation. [d] Coefficients of variation. [e] Square of correlation coefficients.

coefficients of variation, and the square of correlation coefficients for the Freundlich parameters are also included in Table 4. The isosteric heat of adsorption, calculated at a coverage of 80,000 μg of naphthalene/g-activated carbon, was −26 kJ/mol (298−311 K) and −37 kJ/mol (298−328 K). Results were reasonable compared to Weber and Digiano's results[43] for adsorption of 1,2-dichlorobenzene (a compound with a similar K_{ow} value as naphthalene) to activated carbon. Compared to experiment 1, the solid-water distribution coefficient ($K_d = q/C_w$)[42] of naphthalene adsorption to activated carbon is 1000-fold higher than that for "C_{60} large aggregates". For example, at $C_w = 1$ μg/mL, $K_{d,C_{60}} = 10^{2.39}$mL/g, whereas $K_{d,act.carbon} = 10^{5.17}$mL/g at 298 K. By use of the estimated particle size of the "C_{60} large aggregates", (20 to 50) μm, and a density of 1.72 g/cm^3 (reported by SES Research Inc., 6008 West 34th, Houston, TX), the specific surface area is calculated to be from (0.07 to 0.17) m^2/g, which is similar to literature reported values of (0.08 to 0.16) m^2/g[12,16] and similar to what we obtained from particle settling velocities. The specific surface area of the commercial activated carbon in this study was about 1 000 m^2/g, as reported by Calgon Carbon Corp. (Pitts-

Table 5. Experimental Isotherm Data for Naphthalene Adsorption from Electrolyte Solution to "C_{60} Thin Films" and Naphthalene Desorption from "C_{60} Thin Films" into Electrolyte Solution

adsorption		desorption	
C_w / $\mu g \cdot mL^{-1}$	q / $\mu g \cdot g^{-1}$	C_w / $\mu g \cdot mL^{-1}$	q / $\mu g \cdot g^{-1}$
0.71	1015	0.043	352
1.44	1416	0.168	712
2.29	2632	0.819	1553
3.03	3323	3.195	3602
3.79	4985	3.814	4329

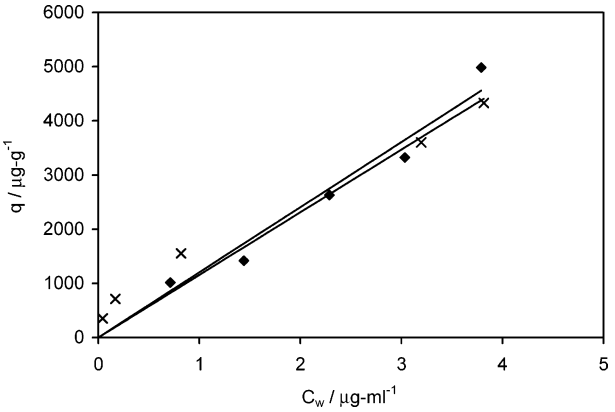

Figure 3. Plot of experimental data of naphthalene adsorption to and desorption from "C_{60} thin films". ◆, Adsorption of naphthalene to "C_{60} thin film"; ×, naphthalene desorption from "C_{60} thin film" into electrolyte solution; solid line, linear isotherms.

burgh, PA). The large difference between the surface areas of "C_{60} large aggregates" and activated carbon is probably a major reason for the difference in the naphthalene adsorption distribution coefficients, on a mass basis.

Adsorption/Desorption of Naphthalene to/from "C_{60} Thin Film". Experiments 3 and 4 were designed to explore the adsorptive properties of C_{60} in a different aggregation form, a thin film. Evaporation of the C_{60}/organic solvent solutions deposited a fairly uniform layer of C_{60} on the walls of the vials. Therefore, these are referred to as "C_{60} thin film" experiments. The equilibrium concentrations of naphthalene adsorption (experiment 3) and desorption (experiment 4) to and from these C_{60} thin films are presented in Table 5. Mean values of coefficients of variation for the final solution-phase naphthalene concentrations was ±0.2%, calculated based on three replicates for each sample. Data are fitted with linear isotherms and are presented in Figure 3. Both adsorption and desorption data were fitted with linear isotherms, K_p (q/C_w) = ($10^{3.08}$ ± 58.40) and ($10^{3.06}$ ± 85.33) mL·g^{-1} for experiments 3 and 4, respectively. Since both the adsorption and desorption isotherms are linear and of similar magnitude, it is suggested that the deposited C_{60} thin films present fairly uniform adsorption sites and stable solid surfaces to the solution. Furthermore, published K_{oc} (organic-carbon-based distribution coefficient) values for naphthalene sorption to various soils and sediments range from ($10^{2.66}$ to $10^{3.17}$) mL/g-OC.[29,44−47] The K_p values for adsorption and desorption of naphthalene obtained in this set of experiments are consistent with K_{oc} values for naphthalene, if C_{60} fullerene carbon is assumed to be similar to soil organic carbon. Whether this agreement is simply a numerical coincidence or suggestive of a common predominant mechanism, e.g., the hydrophobic effect, is not yet known. The stronger adsorption of naphthalene to "C_{60} thin film" than that to the as-received

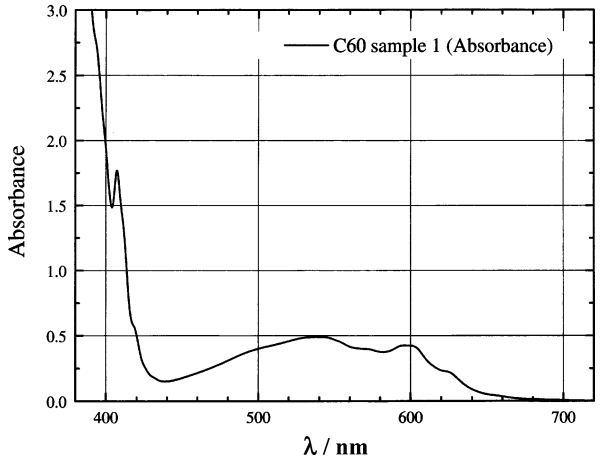

Figure 4. UV−vis absorption spectrum of C_{60} toluene solution. C_{60} was stirred for 2 days before it was dissolved in toluene.

"C_{60} large aggregates" is probably due to increased surface area of the deposited films, although this is not yet proven.

Adsorption/Desorption of Naphthalene to/from "C_{60} Small Aggregates". In experiment 5, C_{60} was dispersed in an aqueous electrolyte solution and stirred for 2 days with a magnetic stirrer. The resulting suspension was turbid with a brownish color. SEM micrographs were taken (not included in this paper) for the resultant C_{60}/electrolyte suspension after 2 days stirring. C_{60} aggregation was clearly observed in the SEM images. The sizes of the C_{60} aggregates were estimated to be (1 to 3) μm in diameter and are referred to as "C_{60} small aggregates".

Many research groups have developed various approaches to prepare C_{60} colloidal particles: sonication of C_{60} toluene solution in water,[19] dispersion of fullerene into water by changing solvents from nonpolar organic solvents to water-mixable polar organic solvents and eventually to water,[48,49] formation of host−guest inclusion complexes with γ-cyclodextrin,[20] formation of micelles using surfactants,[50,51] and generation of C_{60} hydrosol based on the oxidation of C_{60}^- in water-mixable organic solvents.[21] The "C_{60} small aggregates" prepared in this study showed a similar color as observed by Andrievsky et al.[19]

When "C_{60} small aggregates" were dissolved in toluene, the characteristic magenta color of C_{60} appeared. The absorption spectrum (Figure 4) showed a sharp absorption peak at 408 nm, which is characteristic of C_{60}.[50,52−54] Furthermore, there was no evidence of the existence of C_{60} oxide, whose characteristic peak is at 424 nm.[50,52,53,55] Therefore, it is concluded that these "C_{60} small aggregates" are unaltered C_{60} fullerene.

Successive adsorption/desorption experiments were conducted with two separately stirred "C_{60} small aggregates" samples (samples 5.1 and 5.2). Solution-phase naphthalene concentrations and solid-phase naphthalene concentrations at adsorption and desorption equilibrium are presented in Table 6. Mean values of coefficients of variation for the solution-phase naphthalene concentrations was ±0.4%, calculated based on three replicates for each sample. Adsorption data are fitted with Freundlich isotherms (parts a and b of Figure 5). The Freundlich parameters are listed in Table 7, along with the standard deviation, the coefficients of variation, and the square of correlation coefficients. Freundlich equations of $q = 10^{4.28}C_w^{0.45}$ and $q = 10^{4.20}C_w^{0.45}$ are obtained for the two samples, where solid-phase concentrations (q) are in the unit of $\mu g \cdot g^{-1}$ and solution-phase concentrations (C_w) are in the unit of $\mu g \cdot mL^{-1}$. Since the adsorption isotherms for the "C_{60} small

Table 6. Equilibrium Naphthalene Concentrations in Solution and Solid Phases for Naphthalene Adsorption and Desorption to and from "C_{60} Small Aggregates" and the Corresponding Desorption Time (*t*/days)

sample 5.1					sample 5.2				
adsorption		desorption			adsorption		desorption		
C_w	q	t	C_w	q	C_w	q	t	C_w	q
$\mu g \cdot mL^{-1}$	$\mu g \cdot g^{-1}$	days	$\mu g \cdot mL^{-1}$	$\mu g \cdot g^{-1}$	$\mu g \cdot mL^{-1}$	$\mu g \cdot g^{-1}$	days	$\mu g \cdot mL^{-1}$	$\mu g \cdot g^{-1}$
0.021	2348	3	0.168	10929	0.049	3529	2	0.148	8247
0.026	4708	6	0.149	10724	0.082	5601	4	0.117	8106
0.051	5862	8	0.112	10568	0.104	6200	6	0.096	7988
0.181	8500	10	0.088	10448	0.169	7328	8	0.061	7915
0.270	10400	12	0.070	10350	0.300	8428	14	0.053	7716
0.326	11156	14	0.070	10253			16	0.051	7656
		18	0.051	10182			20	0.052	7590
		20	0.045	10119			26	0.026	7560
		24	0.040	10064			29	0.025	7528
		30	0.034	10017			35	0.023	7499
		33	0.028	9979			62	0.013	7483
		39	0.023	9947					
		66	0.011	9932					

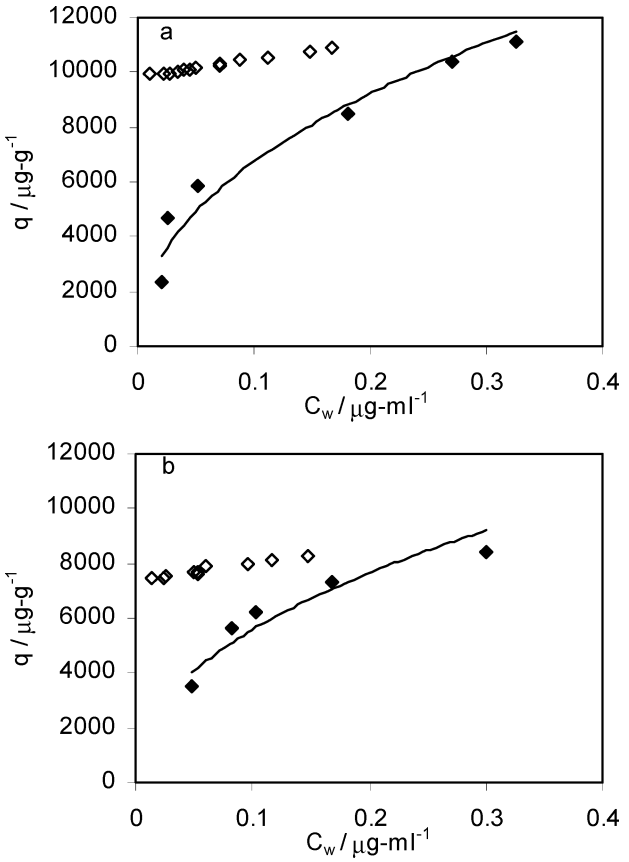

Figure 5. Plot of experimental data of naphthalene adsorption to and desorption from "C_{60} small aggregates". a, Data for 6-step adsorption experiments and 13-step desorption experiments for sample 5.1; b, data for 5-step adsorption experiments and 11-step desorption experiments for sample 5.2; ◆, adsorption data; ◇, desorption data; solid line, Freundlich isotherms.

aggregates" are Freundlich in shape, this suggests that there must be a distribution of adsorption energies on the solid particles in solution,[42,43] which is different from the linear isotherms observed for the "C_{60} large aggregates". Farrell et al.[56] suggested that surface heterogeneities are the most common origin of varying adsorption energies, and this would imply that the effect of the two-day vigorous stirring was to break up the aggregates of the commercial material and, in the process, create disrupted surfaces of varying energies.

Table 7. Freundlich Parameters for Naphthalene Adsorption to "C_{60} Small Aggregates"

sample	K_F [a]	n [b]	R^2 [e]
5.1	$10^{4.28} \pm 10^{3.23}$ [c] (9.0%) [d]	0.45 ± 0.05 [c] (11.1%) [d]	0.95
5.2	$10^{4.20} \pm 10^{3.28}$ (12.0%)	0.45 ± 0.07 (15.5%)	0.90

[a] Freundlich constant. [b] Freundlich exponent. [c] Standard deviation. [d] Coefficients of variation. [e] Square of correlation coefficients.

At $C_w = 1$ μg/mL, the distribution coefficients for naphthalene adsorption to "C_{60} small aggregates" ($K_d = 10^{4.28}$ and $10^{4.20}$ mL·g^{-1}) are about 1.8 log units higher than the corresponding value for the "C_{60} large aggregates" ($10^{2.39}$ mL·g^{-1}), obtained in experiment 1. The specific surface area of "C_{60} small aggregates" is over 1 order of magnitude higher than that of "C_{60} large aggregates", and this may be the reason adsorption of naphthalene to "C_{60} small aggregates" was much stronger.

There is structural similarity of C_{60} fullerene and black carbon, an important component of soil organic carbon. Black carbon consists of single and stacked apolar and polyaromatic sheets.[57,58] By use of the empirical correlation equation of Schwarzenbach et al.,[4,42,59−61] the black-carbon-normalized adsorption coefficient (K_{bc}) for naphthalene is calculated to be $10^{3.93}$ mL·g^{-1}, which is similar to that observed herein with experiment 5.

The desorption isotherms for samples 5.1 and 5.2 are also presented in parts a and b of Figure 5. The desorption isotherms differ considerably from the corresponding adsorption isotherms, suggesting the presence of hysteresis. In these desorption experiments, $K_d = 10^{5.96}$ mL·g^{-1} and $10^{5.75}$ mL·g^{-1} for the last desorption datum point for samples 5.1 or 5.2, respectively. Both final K_d values are more than 1 order of magnitude higher than the last adsorption K_d values.

Many researchers have studied the kinetics of sorption/desorption of hydrophobic organic compounds to/from particles from soils and sediments. For example, the reaction half-life of naphthalene desorption from sediments has been estimated to be (0.74−1.41) h.[62,63] Thus, a period of 60 days was used in the current desorption experiments. The time for various desorption points varied from 2 to 27 days (see Table 6 and Figure 6a) with no apparent effect on the solution concentration, suggesting probable equilibrium. As shown in Figure 6b, after over 60 days desorption period, only about 11% of total naphthalene was desorbed from the "C_{60} small aggregates" (corresponding

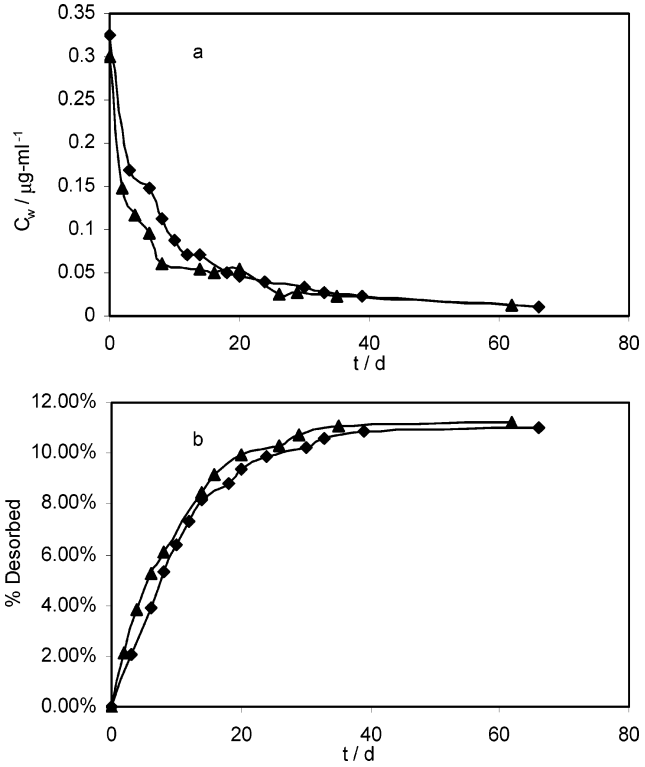

Figure 6. Experimental data for naphthalene desorption from "C_{60} small aggregates". a, Plot of the solution-phase naphthalene concentrations ($C_w/\mu g \cdot ml^{-1}$) vs desorption time (t/days); b, plot of percentage of naphthalene desorbed from C_{60} vs desorption time (t/days); ◆, experimental data points for sample 5.1; ▲, experimental data points for sample 5.2.

Table 8. Change of the Percentage of Naphthalene Amount Desorbed from C_{60} Solid with Desorption Time in Experiment 5 (Desorption of Naphthalene from "C_{60} Small Aggregates")

sample 5.1		sample 5.2	
t (days)	% desorbed	t (days)	% desorbed
3	2.08	2	2.16
6	3.92	4	3.84
8	5.32	6	5.23
10	6.40	8	6.11
12	7.28	14	8.47
14	8.15	16	9.18
18	8.78	20	9.96
20	9.34	26	10.33
24	9.84	29	10.71
30	10.26	35	11.04
33	10.61	62	11.23
39	10.89		
66	11.03		

data are presented in Table 8); i.e., a large fraction of the sorbed naphthalene was resistant to desorption.

By extrapolation of the desorption isotherms to the y axis in Figure 5, intercepts of $10^{4.0}$ and $10^{3.9}$ μg/g are obtained. Converting these intercepts to mole ratio values corresponds to about 1 naphthalene molecule/20 C_{60} molecules. This indicates that, for every 20 C_{60} molecules, there might be 1 naphthalene molecule that cannot be desorbed in any practical time frame.

Sorption/desorption hysteresis of hydrophobic organic compounds in soils or sediments has been studied extensively by numerous researchers, e.g., Karickhoff, Weber, Pignattelo, Kan, and Di Toro et al.[5,22−35] Consistent with many of those studies, a two-compartment irreversible adsorption model has been proposed by Kan et al. to explain the phenomenon of sorption/desorption hysteresis.[32] A reversible compartment and an irreversible compartment have been proposed to be responsible for the complete desorption process. In the reversible compartment, chemicals could be readily and reversibly desorbed, while in the irreversible compartment, desorption of organic compounds could be hindered by soil organic matter.[34] The desorption distribution coefficient in the irreversible compartment was reported to be related directly to soil organic carbon content and has a value of $K_{OC}^{irr} \approx 10^{5.92}$ mL/g-OC for a wide range of hydrophobic organic compounds.[64] This value is in the same order of magnitude as observed desorption K_d values ($10^{5.96}$ mL/g or $10^{5.75}$ mL/g) in this study, indicating the possibility of similar mechanisms for desorption from C_{60} and soil organic carbon materials.

It has been found that many soils or sediments contain various carbonaceous materials such as soot, hard coals, and black carbon, which might contribute significantly to the sorption/desorption hysteresis, or resistant release of organic compounds.[3,4,28,36,65] As more and more carbon nanomaterials are manufactured, they will begin to appear in impacted soils and sediments, and therefore it is important to understand the basic mechanisms of adsorption and desorption of hydrocarbons. If true hysteresis occurs in carbon nanomaterial−hydrocarbon interactions, the impact on environmental fate and transport could be enormous.

Bailey et al.[66] concluded that hysteresis occurs in solids with mesopores (diameters between (20 and 500) Å[56]), and this is usually attributed to "capillary condensation", while hysteresis, which occurs in solids with micropores (diameters < 20 Å[56]), is usually associated with a distortion of the solid with some irreversible change of the pore structure.

The mechanism of pore deformation in carbonaceous materials has been discussed by many researchers. For example, pore dilation in carbonaceous sorbents caused by packing effects of adsorbate molecules,[67] the possible swelling of soot by methanol,[4] and the swelling and irreversible pore deformation of charcoal by benzene aqueous solution have been discussed in the past few years.[36] In many cases, the deformed pore structure did not recover to its original state even when the adsorbate was removed from the adsorbent. Therefore, desorption is often different from adsorption. A minimum requirement for true adsorption/desorption hysteresis to occur is that the adsorbent surface structure can undergo physical−chemical rearrangement upon adsorption; i.e., after adsorbent rearrangement, desorption would take place in a different molecular environment from adsorption.[68]

Among the few studies addressing the adsorptive properties of C_{60} fullerene, Rathousky et al. observed hysteresis in the adsorption/desorption of cyclopentane vapor to C_{60}.[11,12] They explained the observed hysteresis by the penetration of cyclopentane molecules into the bulk of C_{60} crystals and possible entrapment of the adsorbate molecules, as discussed above.

Given the above findings, it is reasonable to believe that the hysteresis observed in this study might be due to deformation of micropores in C_{60} crystals. It is proposed that during the adsorption process, naphthalene molecules probably penetrate into the micropores in C_{60} crystals, which is either due to the crystal defects or the breaking of weak van der Waals bonding between C_{60} molecules. The pressure exerted by adsorbate molecules could cause expansion of some of the pores. If the pore deformation is not completely reversible, some pore entrances, available

for the adsorption, might be blocked in the desorption process leaving some naphthalene molecules entrapped. This may represent the "two-compartment" adsorption processes observed by numerous researchers: the "reversible" adsorption/desorption compartment, where naphthalene adsorbs to the external surfaces of C_{60} crystals and desorbs reversibly, and the "irreversible" adsorption/desorption compartment, where naphthalene penetrates into micropores in C_{60} crystals and may be "entrapped" and thus resistant to desorption. The fact that extensive stirring apparently does not slowly release "entrapped" naphthalene might suggest that the "entrapped" naphthalene could be a new entity, which might no longer be susceptible to desorption in the normal aqueous desorption.

Interestingly, similar "entrapment" was also found in the preparation of C_{60}, where toluene and some other aromatics were commonly used as extraction solvents. Traces of toluene or other solvents were often found entrapped in the C_{60} lattice after removal of bulk toluene.[37]

The existence of C_{60} aggregation in C_{60} aqueous suspension observed in this study may also suggest another possible mechanism for hysteresis observed herein, that is, "capillary condensation". Hysteresis in this system might be associated with "capillary condensation" in mesopores consisting of the interstices between microporous substructures, similar to that discussed by Burgess et al.[69,70] Data presented in this paper demonstrate the presence of sorption/desorption hysteresis; however, additional experiments are necessary to confirm whether a single mechanism or various combined mechanisms are responsible.

Acknowledgment

We gratefully acknowledge the assistance of Professor Bruce Wiesman, Rice University Chemistry Department, for help with the UV−vis spectrophotometry, Professor Mark Weisner and Volodymyr Tarabara, Rice University Civil and Environmental Engineering Department, for running the Coulter particle size measurements, and Dr. Zhenning Gu, Rice University Chemistry Department, for help with SEM measurements. The help and advice of Professor Vicki Colvin, Rice University Chemistry Department, is also acknowledged.

Literature Cited

(1) Kroto, H. W.; Heath, J. R.; O'Brien, S. C.; Curl, R. F.; Smalley, R. E. C60: Buckminsterfullerene. *Nature* **1985**, *318*, 162−163.

(2) Weissenfels, W. D.; Klewer, H. J.; Langhoff, J. Adsorption of Polycyclic Aromatic Hydrocarbons (PAHs) by Soil Particles: Influence on Biodegradability and Biotoxicity. *Appl. Microbiol. Biotechnol.* **1992**, *36*, 689−696.

(3) Chiou, C. T.; Kile, D. E. Deviation from Sorption Linearity on Soils of Polar and Nonpolar Organic Compounds at Low Relative Concentrations. *Environ. Sci. Technol.* **1998**, *32* (3), 338−343.

(4) Bucheli, T. D.; Gustafsson, O. Quantification of the Soot−Water Distribution Coefficient of PAHs Provides Mechanistic Basis for Enhanced Sorption Observations. *Environ. Sci. Technol.* **2000**, *34*, 5144−5151.

(5) McGroddy, S. E.; Farrington, J. W.; Gschwend, P. M. Comparison of the in situ and Desorption of Sediment−Water Partitioning of Polycyclic Aromatic Hydrocarbons and Polychlorinated Biphenyls. *Environ. Sci. Technol.* **1996**, *30* (1), 172−177.

(6) Gustafsson, O.; Haghseta, F.; Chan, C.; Macfarlane, J.; Gschwend, P. M. Quantification of the Dilute Sedimentary Soot Phase: Implications for PAH Speciation and Bioavailability. *Environ. Sci. Technol.* **1997**, *31*, 203−209.

(7) Pirrier, M. A.; Bordelon, B. R.; Laseter, J. L. Adsorption and Concentration of Dissolved Carbon-14 DDT by Coloring Colloids in Surface H_2O. *Environ. Sci. Technol.* **1972**, *6*, 1033−1035.

(8) McCarthy, J. F.; Jimenez, B. D. Interaction between Polycyclic Aromatic Hydrocarbons and Dissolved Humic Material: Binding and Dissociation. *Environ. Sci. Technol.* **1985**, *19*, 1072−1076.

(9) Kan, A. T.; Tomson, M. B. Groundwater Transport of Hydrophobic Organic Compounds in the Presence of Dissolved Organic Matter. *Environ. Toxicol. Chem.* **1990**, *9*, 253−263.

(10) Kaneko, K.; Ishii, C.; Arai, T.; Suematsu, H. Defect-Associated Microporous Nature of Fullerene C_{60} Crystals. *J. Phys. Chem.* **1993**, *97*, 6764−6766.

(11) Rathousky, J.; Starek, J.; Zukal, A.; Kratschmer, W. Uptake of Cyclopentane Vapors in a Fullerite Powder. *Fullerene Sci. Technol.* **1993**, *1* (4), 575−582.

(12) Rathousky, J.; Zukal, A. Adsorption of Krypton and Cyclopentane on C_{60}: An Experimental Study. *Fullerene Sci. Technol.* **2000**, *8* (4 and 5), 337−350.

(13) Sing, K. S. W. Physisorption of Gases by Carbon Blacks. *Carbon* **1994**, *32*, 1311−1317.

(14) Abraham, M. H.; Du, C. M.; Grate, J. W.; McGill, R. A.; Shuely, W. J. Fullerene as an Adsorbent for Gases and Vapors. *J. Chem. Soc., Chem. Commun.* **1993**, *24*, 1863−1864.

(15) Davydov, V. Y.; Filatova, G. N.; Khrustaleva, N. M.; Roshchina, T. M. Comparative Study of Adsorption Properties of Fullerenes C_{60} and C_{70} Crystals. *Electrochem. Soc. Proc. 95* **1995**, *10*, 1610−1624.

(16) Davydov, V. Y.; Kalashnikova, E. V. Thermodynamic Characteristics of Adsorption of Organic Compounds on Molecular Crystals C_{60}. *Electrochem. Soc. Proc. 98* **1998**, (8), 717−730.

(17) Mchedlov-Petrossyan, N. O.; Klochkov, V. K.; Andrievsky, G. V.; Ishchenko, A. A. Interaction between Colloidal Particles of C_{60} Hydrosol and Cationic Dyes. *Chem. Phys. Lett.* **2001**, *341*, 237−244.

(18) Ballesteros, E.; Gallego, M.; Valcarcel, M. Analytical Potential of Fullerene as Adsorbent for Organic and Organometallic Compounds from Aqueous Solutions. *J. Chromatogr. A* **2000**, *869*, 101−110.

(19) Andrievsky, G. V.; Kosevich, M. V.; Vovk, O. M.; Shelkovsky, V. S.; Vashchenko, L. A. On the Production of an Aqueous Colloidal Solution of Fullerenes. *J. Chem. Soc., Chem. Commun.* **1995**, 1281−1282.

(20) Andersson, T.; Nilsson, K.; Sundahl, M.; Westman, G.; Wennerstrom, O. C_{60} Embedded in γ-Cyclodextrin: A Water-Soluble Fullerene. *J. Chem. Soc., Chem. Commun.* **1992**, *8*, 604−607.

(21) Wei, X.; Wu, M.; Qi, L.; Xu, Z. Selective Solution-Phase Generation and Oxidation Reaction of C_{60}^{n-} (n = 1, 2) and Formation of an Aqueous Colloical Solution of C_{60}. *J. Chem. Soc., Perkin Trans. 2* **1997**, 1389−1393.

(22) Karickhoff, S. W.; Morris, K. R. Sorption Dynamics of Hydrophobic Pollutants in Sediment Suspensions. *Environ. Toxicol. Chem.* **1985**, *4* (4), 469−479.

(23) Huang, W.; Weber, W. J. J. A Distributed Reactivity Model for Sorption by Soils and Sediments: 10. Relationships between Desorption, Hysteresis, and the Chemical Characteristics of Organic Domains. *Environ. Sci. Technol.* **1997**, *31* (9), 2562−2569.

(24) Huang, W.; Yu, H.; Weber, W. J. J. Hysteresis in the Sorption and Desorption of Hydrophobic Organic Contaminants by Soils and Sediments. 1. A Comparative Anylysis of Experimental Protocols. *J. Contam. Hydrol.* **1998**, *31*, 129−148.

(25) Weber, W. J. J.; Huang, W.; Yu, H. Hysteresis in the Sorption and Desorption of Hydrophobic Organic Contaminants by Soils and Sediments. 2. Effects of Soil Organic Matter Heterogeneity. *J. Contam. Hydrol.* **1998**, *31*, 149−165.

(26) Pignatello, J. J.; Huang, L. Q. Sorptive Reversibility of Atrazine and Metolachlor Residues in Field Soil Samples. *J. Environ. Qual.* **1991**, *20* (1), 222−228.

(27) Pignatello, J. J.; Xing, B. Mechanisms of Slow Sorption of Organic Chemicals to Natural Particles. *Environ. Sci. Technol.* **1996**, *30* (1), 1−11.

(28) Xia, G.; Pignatello, J. J. Detailed Sorption Isotherms of Polar and Apolar Compounds in a High-Organic Soil. *Environ. Sci. Technol.* **2001**, *35*, 84−94.

(29) Kan, A. T.; Fu, G.; Tomson, M. B. Adsorption/Desorption Hysteresis in Organic Pollutant and Soil/Sediment Interaction. *Environ. Sci. Technol.* **1994**, *28*, 859−867.

(30) Fu, G.; Kan, A. T.; Tomson, M. B. Adsorption and Desorption Hysteresis of PAHs in Surface Sediment. *Environ. Toxicol. Chem.* **1994**, *13* (10), 1559−1567.

(31) Chen, W.; Kan, A. T.; Fu, G.; Vignona, L. C.; Tomson, M. B. Adsorption−Desorption Behaviors of Hydrophobic Organic Compounds in Sediments of Lake Charles, Louisiana, USA. *Environ. Toxicol. Chem.* **1999**, *18* (8), 1610−1616.

(32) Kan, A. T.; Fu, G.; Hunter, M.; Chen, W.; Ward, C. H.; Tomson, M. B. Irreversible Adsorption of Neutral Organic Hydrocarbons−Experimental Observations and Model Predictions. *Environ. Sci. Technol.* **1998**, *32*, 892−902.

(33) Chen, W.; Kan, A. T.; Tomson, M. B. Irreversible Adsorption of Chlorinated Benzenes to Natural Sediments: Implications for Sediment Quality Criteria. *Environ. Sci. Technol.* **2000**, *34*, 385−392.

(34) Kan, A. T.; Chen, W.; Tomson, M. B. Desorption Kinetics of Neutral Hydrophobic Organic Compounds from Field-Contaminated Sediment. *Environ. Pollut.* **2000**, *108*, 81−89.

(35) Di Toro, D. M.; Horzempa, L. M. Reversible and Resistant Components of PCB Adsorption−Desorption: Isotherms. *Environ. Sci. Technol.* **1982**, *16* (9), 594−602.
(36) Braida, W. J.; Pignatello, J. J.; Lu, Y.; Ravikovitch, P. I.; Neimark, A. V.; Xing, B. Sorption Hysteresis of Benzene in Charcoal Particles. *Environ. Sci. Technol.* **2003**, *37* (2), 409−417.
(37) Taylor, R. *Lecture Notes on Fullerene Chemistry, A Handbook for Chemists*; Imperial College Press: London, 1999.
(38) Jones, K. D.; Tiller, C. L. Effect of Solution Chemistry on the Extent of Binding of Phenanthrene by a Soil Humic Acid: A Comparison of Dissolved and Clay-Bound Humic. *Environ. Sci. Technol.* **1999**, *33*, 580−587.
(39) Ogram, A. V.; Jessup, R. E.; Ou, L. T.; Rao, P. S. Effects of Sorption on Biological Degradation Rates of (2,4-Dichlorophenoxy) Acetic Acid in Soils. *Appl. Environ. Microbiol.* **1985**, *49* (3), 582−587.
(40) Murphy, E. M.; Zachara, J. M.; Smith, S. C. Influence of Mineral-Bound Humic Substances on the Sorption of Hydrophobic Organic Compounds. *Environ. Sci. Technol.* **1990**, *24*, 1507−1516.
(41) Conte, P.; Zena, A.; Pilidis, G.; Piccolo, A. Increased Retention of Polycyclic Aromatic Hydrocarbons in Soils Induced by Soil Treatment with Humic Substances. *Environ. Pollut.* **2001**, *112*, 27−31.
(42) Schwarzenbach, R. P.; Gschwend, P. M.; Imboden, D. M. *Environmental Organic Chemistry*, 2nd ed.; John Wiley & Sons: Hoboken, New Jersey, 2003.
(43) Weber, W. J. J.; Digiano, F. A. *Process Dynamics in Environmental Systems*; John Wiley & Sons: New York, 1996.
(44) Kan, A. T.; Tomson, M. B. Effect of pH Concentration on the Transport of Naphthalene in Saturated Aquifer Media. *J. Contam. Hydrol.* **1990**, *5* (3), 235−251.
(45) Karickhoff, S. W.; Brown, D. S.; Scott, T. A. Sorption of Hydrophobic Pollutants on Natural Sediments. *Water Res.* **1979**, *13*, 241−248.
(46) Lyman, W. J.; Reehl, W. F.; Rosenblatt, D. H. *Handbook of Chemical Property Estimation Methods*; McGraw-Hill: New York, 1982.
(47) Abdul, A. S.; Gibson, T. L. Equilibrium Batch Experiments with Six Polycyclic Aromatic Hydrocarbons and Two Aquifer Materials. *Hazard. Waste Hazard. Mater.* **1986**, *3* (2), 125−137.
(48) Scrivens, W. A.; Tour, J. M.; Creek, K. E.; Pirisi, L. Synthesis of ^{14}C-Labeled C_{60}, Its Suspension in Water, and Its Uptake by Human Keratinocytes. *J. Am. Chem. Soc.* **1994**, *116*, 4517−4518.
(49) Alargova, R. G.; Deguchi, S.; Tsujii, K. Stable Colloidal Dispersions of Fullerenes in Polar Organic Solvents. *J. Am. Chem. Soc.* **2001**, *123*, 10460−10467.
(50) Beeby, A.; Eastoe, J.; Heenan, R. K. Solubilization of C_{60} in Aqueous Micellar Solution. *J. Chem. Soc., Chem. Commun.* **1994**, 173−175.
(51) Bensasson, R. V.; Bienvenue, E.; Dellinger, M.; Leach, S.; Seta, P. C_{60} in Model Biological Systems. A UV−vis Absorption Study of Solvent-Dependent Parameters and Solute Aggregation. *J. Phys. Chem.* **1994**, *98*, 3492−3500.
(52) Heymann, D.; Bachilo, S. M.; Weisman, R. B.; Cataldo, F.; Fokkens, R. H.; Nibbering, N. M. M.; Vis, R. D.; Chibante, L. P. F. $C_{60}O_3$, a Fullerene Ozonide: Synthesis and Dissociation to $C_{60}O$ and O_2. *J. Am. Chem. Soc.* **2000**, *122*, 11473−11479.
(53) Weisman, R. B.; Heymann, D.; Bachilo, S. M. Synthesis and Characterization of the "Missing" Oxide of C_{60}: [5,6]-Open $C_{60}O$. *J. Am. Chem. Soc.* **2001**, *123*, 9720−9721.
(54) Bachilo, S. M.; Benedetto, A. F.; Weisman, R. B. Triplet-State Dissociation of C_{120}, the Dimer of C_{60}. *J. Phys. Chem. A* **2001**, *105*, 9845−9850.
(55) Creegan, K. M.; Robbins, J. L.; Robbins, W. K.; Millar, J. M.; Shetwood, R. D.; Tindall, P. J.; Cox, D. M.; Smith, A. B.; McCauley, J. P.; Jones, D. R.; Gallagher, R. Synthesis and Characterization of $C_{60}O$, the First Fullerene Epoxide. *J. Am. Chem. Soc.* **1992**, *114* (3), 1103−1105.
(56) Farrell, J.; Reinhard, M. Desorption of Halogenated Organics from Model Solids, Sediments, and Soil under Unsaturated Conditions. 1. Isotherms. *Environ. Sci. Technol.* **1994**, *28*, 53−62.
(57) Goldberg, E. D. *Black Carbon in the Environment*; John Wiley & Sons: New York, 1985.
(58) Gustafsson, O.; Bucheli, T. D.; Kukulska, Z.; Andersson, M.; Largeau, C.; Rouzaud, J.-N.; Reddy, C. M.; Eglinton, T. I. Evaluation of a Protocol for the Quantification of Black Carbon in Sediments. *Global Biogeochem. Cycles* **2001**, *15* (4), 881−890.
(59) Xia, G.; Ball, W. P. Adsorption-Partitioning Uptake of Nine Low-Polarity Organic Chemicals on a Natural Sorbent. *Environ. Sci. Technol.* **1999**, *33* (2), 262−269.
(60) Gawlik, B. M.; Sotiriou, N.; Feicht, E. A.; Schulte-Hostede, S.; Kettrup, A. Alternatives for the Determination of the Soil Adsorption Coefficient, Koc, of Nonionic Organic Compounds. A Review. *Chemosphere* **1997**, *34* (12), 2525−2551.
(61) Accardi-Dey, A.; Gschwend, P. M. Assessing the Combined Roles of Natural Organic Matter and Black Carbon as Sorbents in Sediments. *Environ. Sci. Technol.* **2002**, *36* (1), 21−29.
(62) Karickhoff, S. W. *Sorption Kinetics of Hydrophobic Pollutants in Natural Sediments*; Baker, R. A., Ed.; Ann Arbor Science Publishers: Ann Arbor, MI, 1980.
(63) Karickhoff, S. W.; Morris, K. R. Impact of Tubificid Oligochaetes on Pollutant Transport in Bottom Sediments. *Environ. Sci. Technol.* **1985**, *19* (1), 51−56.
(64) Chen, W.; Kan, A. T.; Newell, C. J.; Moore, E.; Tomson, M. B. More Realistic Soil Cleanup Standards with Dual-Equilibrium Desorption. *Groundwater* **2002**, *40* (2), 153−164.
(65) McGroddy, S. E.; Farrington, J. W. Sediment Porewater Partitioning of Polycyclic Aromatic Hydrocarbons in Three Cores from Boston Harbor, Massachusetts. *Environ. Sci. Technol.* **1995**, *29* (6), 1542−1550.
(66) Bailey, A.; Cadenhead, D. A.; Davies, D. H.; Everett, D. H.; Miles, A. J. Low-Pressure Hysteresis in the Adsorption of Organic Vapors by Porous Carbons. *Trans. Faraday Soc.* **1971**, *67*, 231−243.
(67) Olivier, J. P. Improving the Models Used for Calculating the Size Distribution of Micropore Volume of Activated Carbons from Adsorption Data. *Carbon* **1998**, *36* (10), 1469−1472.
(68) Adamson, A. W.; Gast, A. P. *Physical Chemistry of Surfaces*, 6th ed.; John Wiley & Sons: New York, 1997.
(69) Burgess, C. G. V.; Everett, D. H.; Nuttall, S. Adsorption Hysteresis in Porous Materials. *Pure Appl. Chem.* **1989**, *61* (11), 1845−1852.
(70) Andrievsky, G. V.; Klochkov, V. K.; Bordyuh, A. B.; Dovbeshko, G. I. Comparative Analysis of Two Aqueous-Colloidal Solutions of C_{60} Fullerene with Help of FTIR Reflectance and UV−vis Spectroscopy. *Chem. Phys. Lett.* **2002**, *364*, 8−17.

Received for review November 17, 2003. Accepted February 11, 2004. The financial support of the Center for Biological and Environmental Nanotechnology at Rice University and the U.S. EPA Hazardous Substance Research Center/South & Southwest Region is greatly appreciated.

JE030247M